HHS Public Access

Author manuscript

Biochim Biophys Acta. Author manuscript; available in PMC 2018 January 01.

Published in final edited form as:

Biochim Biophys Acta. 2017 January ; 1863(1): 33–42. doi:10.1016/j.bbadis.2016.10.009.

Therapeutic Relevance of mTOR Inhibition in Murine Succinate Semialdehyde Dehydrogenase Deficiency (SSADHD), a Disorder of GABA Metabolism[a]

KR Vogel[1], **GR Ainslie**[1], **EEW Jansen**[2], **GS Salomons**[2], and **KM Gibson**[1,a]

[1]Division of Experimental and Systems Pharmacology, College of Pharmacy, Washington State University, Spokane WA, USA [2]Metabolic Unit, Department of Clinical Chemistry, VU University Medical Center, Neuroscience Campus, Amsterdam, The Netherlands

Abstract

Aldehyde dehydrogenase 5a1-deficient (*aldh5a1*$^{-/-}$) mice, the murine orthologue of human succinic semialdehyde dehydrogenase deficiency (SSADHD), manifest increased GABA (4-aminobutyric acid) that disrupts autophagy, increases mitochondria number, and induces oxidative stress, all mitigated with the mTOR (mechanistic target of rapamycin) inhibitor rapamycin [1]. Because GABA regulates mTOR, we tested the hypothesis that *aldh5a1*$^{-/-}$ mice would show altered levels of mRNA for genes associated with mTOR signaling and oxidative stress that could be mitigated by inhibiting mTOR. We observed that multiple metabolites associated with GABA metabolism (γ-hydroxybutyrate, succinic semialdehyde, D-2-hydroxyglutarate, 4,5-dihydrohexanoate) and oxidative stress were significantly increased in multiple tissues derived from *aldh5a1*$^{-/-}$ mice. These metabolic perturbations were associated with decreased levels of reduced glutathione (GSH) in brain and liver of *aldh5a1*$^{-/-}$ mice, as well as increased levels of adducts of the lipid peroxidation by-product, 4-hydroxy-2-nonenal (4-HNE). Decreased liver mRNA levels for multiple genes associated with mTOR signaling and oxidative stress parameters were measured in *aldh5a1*$^{-/-}$ mice, and several were significantly improved with the administration of mTOR inhibitors (Torin 1/Torin 2). Western blot analysis of selected proteins corresponding to oxidative stress transcripts (glutathione transferase, superoxide dismutase, peroxiredoxin 1) confirmed gene expression findings. Our data provide additional preclinical evidence for the potential therapeutic efficacy of mTOR inhibitors in SSADHD.

[a]Abbreviations employed: GABA, gamma-aminobutyric acid; Tor 1, Torin 1; Tor 2, Torin 2; SSADH, succinic semialdehyde dehydrogenase; SSADHD, succinic semialdehyde dehydrogenase deficiency; *aldh5a1*, aldehyde dehydrogenase 5a1 (identical to succinic semialdehyde dehydrogenase)

[a]Correspondence: Division of Experimental and Systems Pharmacology, College of Pharmacy, Washington State University, Pharmaceutical and Basic Sciences Building Room 347, 412 E. Spokane Falls Blvd, Spokane, WA, USA; phone 509 358 7954; mike.gibson@wsu.edu.

Keywords

GABA; succinic semialdehyde dehydrogenase deficiency; mTOR; torin 1; torin 2; oxidative stress

1. Introduction

Inhibitory GABA derives from the primary excitatory neurotransmitter, glutamate, via decarboxylation catalyzed by glutamate decarboxylase (*GAD*). GABA is metabolized to succinic acid via GABA-transaminase (GABA-T; Fig. 1) and succinic semialdehyde dehydrogenase (ALDH5A1; aldehyde dehydrogenase 5a1=succinic semialdehyde dehydrogenase (SSADH)). Mendelian disorders of both GABA-T and ALDH5A1 exist [2–4]. ALDH5A1 deficiency (also referred to as succinic semialdehyde dehydrogenase deficiency (SSADHD)) presents with a non-specific neurological phenotype encompassing developmental delay, expressive language impairment, variable epilepsy [5, 6], and neuropsychiatric problems (i.e. ADHD, OCD, aggression). The biochemical hallmarks of SSADHD include accumulation of glutamate, GABA and the GABA-derivative γ-hydroxybutyrate (GHB) [7] in physiological fluids, the latter an intermediate with a complex pharmacology and the cardinal physiological biomarker of SSADHD [8] (Fig. 1). Our understanding of the pathophysiology of SSADHD has evolved from studies in the murine model [9]. This model was derived by standard cre-lox recombination, with deletion of exon 7 containing a catalytic cysteine residue [10]. Metabolically, *aldh5a1*$^{-/-}$ mice represent a valid phenocopy of the human disease, with elevations of both GABA and GHB in tissues and biofluids [11]. *Aldh5a1*$^{-/-}$ mice manifest a seizure phenotype, including progression from absence to tonic-clonic seizures to lethal status epilepticus by day of life (DOL) 25 [12]. Accordingly, metabolic or other studies, as well as therapeutic considerations, must be implemented within the first 2–3 weeks of life.

Lakhani and coworkers recently defined a role for GABA in autophagy in yeast. High levels of GABA impaired both mitophagy and pexophagy [1]. These findings were reproduced in *aldh5a1*$^{-/-}$ mice. Intervention with the mTOR inhibitor rapamycin resulted in normalization of elevated hepatic pS6 (a kinase linked to mTOR function), superoxide dismutase (SOD), and mitochondrial numbers. Comparable impairments of autophagy have been identified associated with vigabatrin intervention, an antiepileptic employed for treatment of infantile spasms which irreversibly inactivates GABA-T and elevates GABA [13]. Neurophysiological data also suggests synergistic actions between GABA and mTOR. For example, mTOR mediates synaptic regulation through modulation of miniature inhibitory postsynaptic currents that are GABA-mediated [14], and hyperactive mTOR elevates evoked synaptic responses in both glutamatergic and GABAergic neurons. Moreover, mTOR may be activated by calcium signaling mediated by $GABA_B$ receptors [15]. The preceding observations suggest that mTOR is an appropriate therapeutic target for diseases with altered GABA homeostasis.

Here, we extend our characterization of mTOR inhibitors as a therapeutic consideration for SSADHD, employing *aldh5a1*$^{-/-}$ mice as the experimental platform. Initially, we characterized elevations of GABA-associated metabolites in brain, liver and kidney of

aldh5a1$^{-/-}$ mice vs. *aldh5a1*$^{+/+}$ mice, including GABA, GHB, D-2-HG, SSA, and DHHA (see Fig. 1). The majority of these metabolites induce oxidative stress when administered individually to rodents [16–20]. We then confirmed significant depletion of reduced glutathione (GSH) in brain and liver of *aldh5a1*$^{-/-}$ mice [16], and extended those findings by documenting significant depletion of total GSH in extracts of RBCs (red blood cells) derived from patients with SSADHD [21]. Additionally, we demonstrated elevated 4-HNE conjugates in extracts of brain derived from *aldh5a1*$^{-/-}$ as compared to *aldh5a1*$^{+/+}$ mice, a relevant finding since SSADH is the primary aldehyde dehydrogenase responsible for further oxidation of 4-HNE in rodent brain [22]. These metabolic evaluations set the stage for a novel, comprehensive characterization of mRNA levels associated with genes involved in both mTOR signaling and the maintenance of intracellular oxidation-reduction potential, and the potential beneficial effect of agents which inhibit mTOR signaling (Tor 1/Tor 2) on these mRNA levels and selected related proteins.

2. Methods

2.1 Animal and human studies

All animal procedures were approved by the Washington State University IACUC (protocol 0432 and 0476). *Aldh5a1*$^{-/-}$ mice were generated via harem breeding (*aldh5a1*$^{+/-}$ females (2) x *aldh5a1*$^{+/-}$ male). This strain, developed in the Gibson laboratory, is syngeneic on the C57Bl background, and has been backcrossed to wild-type C57Bl stock yearly for 10 years. The model is a complete null for *aldh5a1* activity due to the loss of exon 7 containing an active site cysteine required for activity [10]. At birth, offspring are subjected to tail snip for production of genomic DNA. The latter is employed for nested 3-primer PCR genotyping [10]. All mice were maintained on a standard 12 hour light/dark schedule, with ad-libitum delivery of standard mouse chow (Teklad 2018, Harlan Laboratories). Mice were sacrificed by 1–2 minute exposure to carbon dioxide followed by cervical dislocation. Tissues were immediately dissected on an ice-cold glass plate followed by rapid immersion into dry ice/ethanol and storage at −80 °C. Whole blood was obtained from patients with SSADHD and control individuals with informed consent (IRB 12678). RBCs were isolated by centrifugation on Ficoll-Hypaque (Sigma-Aldrich, St. Louis, MO, USA), and pelleted RBCs washed with PBS and stored at −80 °C until analysis.

2.1 Reagents

Torin 1 and 2 were obtained from Tocris Biosciences (Bristol, United Kingdom), and were dissolved in DMSO at 25mg/mL. Stock solutions were diluted in PBS and administered to mice via intraperitoneal injection commencing at day of life (DOL) 10. Antibodies were purchased from ThermoFisher Scientific (Waltham MA) except GAPDH (Santa Cruz Biotechnologies; Santa Cruz CA). The final DMSO percentage administered to animals was less than 0.1%. Both *aldh5a1*$^{+/+}$ and untreated *aldh5a1*$^{-/-}$ mice received vehicle control injections.

2.2 Metabolic studies

Metabolites quantified in liver, kidney and brain derived from *aldh5a1*$^{-/-}$ and *aldh5a1*$^{+/+}$ mice included GHB, GABA, succinic semialdehyde (SSA), D-2-hydroxyglutaric acid (D-2-

HG), and 4,5-dihydroxyhexanoic acid (DHHA) (Fig. 1). Animals were 17–20 days of age, and of mixed gender. Metabolites were quantified in tissues stored at −80°C until work-up. Tissues were homogenized at 1:10 w/v in 3% sulfosalicylic acid and supernatants obtained by centrifugation. Tissues were harvested from n=8 each *aldh5a1*$^{+/+}$ and *aldh5a1*$^{-/-}$ mice that were age-matched littermates of mixed gender. Metabolite quantitation in tissue supernatants was performed using isotope dilution methodology. GHB was measured using gas chromatography-mass spectrometry (GCMS) and $^{2}H_{6}$-GHB as internal standard [23]. GABA was measured by electron-capture negative-ion mass fragmentography employing $^{13}C_{2}$-GABA as internal standard [24]. SSA was quantified as the dinitrophenylhydrazine derivative employing liquid chromatography-tandem mass spectrometry (LC-MS/MS) and $^{13}C_{4}$-SSA as internal standard [25]. D-2-HG was quantified as described [26] using chiral separation. In brief, D-2-HG was separated from L-2-hydroxyglutaric acid employing stable-isotope-dilution liquid chromatography-tandem mass spectrometry following derivatization with diacetyl-L-tartaric anhydride. The method for quantitation of DHHA was similar to that for GHB and employed ($^{2}H_{3}$-*CH*$_{3}$)-4,5-DHHA (synthesized in-house) as internal standard [27]. Metabolite concentrations were standardized to wet weight of tissue. Metabolic analyses were performed in whole organs.

2.3 Reduced glutathione (GSH) and 4-hydroxy-2-nonenal (4-HNE) adducts

GSH and 4-HNE adducts were quantified in brain and liver obtained from n=8 each *aldh5a1*$^{+/+}$ and *aldh5a1*$^{-/-}$ mice that were age-matched littermates of mixed gender. GSH is the major tripeptide intracellular antioxidant, while 4-HNE represents an α,β-unsaturated hydroxyalkenal produced during cellular lipid peroxidation, the primary unsaturated hydroxyalkenal formed during lipid peroxidation. 4-HNE is short-lived due to the presence of 3 reactive groups, including aldehyde, double-bond and hydroxyl-moiety (Fig. 1).

2.3.1 Reduced glutathione (GSH)—Reduced GSH was quantified using a modification of the procedure by Moore and coworkers [28].

2.3.2. Total GSH in extracts of RBCs from patients with SSADHD—RBCs derived from patients with SSADHD (n=9) and control individuals (unaffected siblings of patients, parents and unrelated controls; n=7, not age- or gender-matched) were isolated with standard Ficoll gradient centrifugation and quantified for oxidized, reduced and total GSH by colorimetric assay obtained from Trevigen (Gaithersburg, MD) using manufacturer's suggested protocol.

2.3.3 Quantitation of 4-HNE adducts—Adducts of 4-HNE were quantified in brain and liver derived from n=8 each *aldh5a1*$^{+/+}$ and *aldh5a1*$^{-/-}$ mice that were age-matched littermates of mixed gender. The protocol employed a colorimetric ELISA assay from CellBiolabs (San Diego, CA). A BSA-4-HNE standard contained in the ELISA kit was employed to obtain standard curves for quantitation.

2.4 Quantitation of mRNA levels

RNA was prepared by pooling liver/brain tissues (whole organs) with n=4 for wild-type (WT) and mutant (MUT) mice, day of life (DOL) 21, n=2 survivors for Tor1 (5 mg/kg daily;

DOL 50); and n=1 survivor for 5mg/kg Tor2 (DOL 50). Samples were homogenized with TRIzol® (Invitrogen). Samples for Tor 1 and 2 were taken from *aldh5a1*$^{-/-}$ mice that were 50 days old, which is highly significant in view of uniform lethality by day of life (DOL) 25 in the absence of therapy [10, 29]. Accordingly, parallel untreated *aldh5a1*$^{-/-}$ mice were not available for comparison to treated mice at the DOL 50 timepoint. Homogenates were chloroform extracted, and RNA was precipitated with isopropanol and ethanol followed by brief air drying and reconstitution in water. RNA was quantified via absorbance and purity assessed using 260 nm/280 nm absorbance ratio (> 1.8). iScript mastermix (Biorad, Hercules CA) was employed to generate cDNA employing an Eppendorf mastercycler per manual instructions with 1 μg RNA/20 μL reaction. Sybr green (Biorad) reactions were prepared as a master mix with 50 ng of cDNA/10 μl/well pipetted into prearrayed and validated (per MIQE guidelines; [30]) mTOR pathway analysis plates and oxidative stress arrays (M394 PrimePCR^{TM} SABioscience). A BioRad CFX384 real-time PCR with BioRad CFX manager v3.0 software was employed for data acquisition, normalization, expression and statistical analysis with significance set at $p<0.05$ based upon two replicates per group. Statistical analysis for the arrays employed a one-way ANOVA with post-hoc Bonferroni *t*-test correction, as described [31]. *Aldh5a1*$^{-/-}$ mice (treated or untreated) were compared to the expression level detected for untreated, control *aldh5a1*$^{+/+}$ mice (expression set to 1.0). The Biorad website describes for the prime PCR how the relevant genes have been compiled for expression arrays: http://www.bio-rad.com/en-us/prime-pcr-assays/pathway/primepcr-pathways

2.5 Western blot analyses

Liver samples (whole organs) were mechanically homogenized in cold RIPA buffer with antiprotease and antiphosphatase tablets (Roche, Pleasanton CA), sonicated for five minutes in an ice bath, and quantitated for total protein using the Pierce bicinchoninic acid (BCA) colorimetric protein assay (Abs 562 nm). Samples and BSA standards were read on a BioTek Synergy 4 microplate reader and extrapolated with GraphPad Prism 6. Sample homogenates were diluted in PBS, lithium dodecyl sulfate (LDS) sample buffer and 50 mM dithiothreitol (DTT) reducing agent to a loading concentration of 50 μg/well and incubated at 70°C for 10 minutes, vortexed, and placed immediately on ice. 30 μL was loaded into Bolt 4–12% Bis-Tris pre-cast polyacrylamide gels and electrophoresed for 35 minutes at a constant 165 volts in MES running buffer. Protein was transferred to nitrocellulose using the iBlot2® transfer system, blocked, and probed with alkaline phosphatase conjugated secondary antibody. Protein bands were detected using chemiluminescent CDP-Star® Substrate with Nitro-II Enhancer (Novex) on a BioRad gel documentation imager and analyzed by normalization to either GAPDH or vinculin (loading controls).

3. Results

3.1 Metabolic abnormalities related to the GABA pathway in *aldh5a1*$^{-/-}$ mice

Concentrations of GHB, GABA, SSA, D-2-HG and DHHA in extracts of brain, liver and kidney were obtained for *aldh5a1*$^{+/+}$ and *aldh5a1*$^{-/-}$ mice (Figs. 2A–2E). Values were (all nmol/mg tissue, n=8 mice of each genotype, mean ± SEM, *aldh5a1*$^{-/-}$ mice and *aldh5a1*$^{+/+}$ mice in parentheses): GHB in liver, 481 ± 133 (5.7 ± 0.8); kidney, 514 ± 68 (12 ± 2.5);

brain, 510 ± 65 (1.9 ± 0.2); GABA in liver, 510 ± 46 (31 ± 4); kidney, 651 ± 14 (54 ± 16); brain, 8915 ± 167 (2109 ± 37); SSA in liver, 15 ± 1.4 (5.4 ± 0.5); kidney, 21 ± 1.4 (14 ± 0.6); brain, 23 ± 3 (2.8 ± 1.2); D-2-HGA in liver, 1857 ± 213 (18 ± 4); kidney, 1191 ± 101 (37 ± 2.8); brain 85 ± 7.5 (28 ± 1.3); DHHA in liver, 5.7 ± 0.6 (none detected); kidney, 56 ± 8.3 (0.5 ± 0.2); brain, 80 ± 9.6 (0.2 ± 0.2). Concentrations of all metabolites were significantly increased in tissues of *aldh5a1*$^{-/-}$ mice as compared to *aldh5a1*$^{+/+}$ ($p<0.01$, two tailed *t* test).

3.2 Glutathione levels in mouse tissues and red blood cells derived from patients with SSADHD

Reduced glutathione (GSH) was quantified in extracts of brain and liver derived from *aldh5a1*$^{-/-}$ and *aldh5a1*$^{+/+}$ mice (n=8 each genotype, mixed gender, age-matched, *aldh5a1*$^{+/+}$ with *aldh5a1*$^{-/-}$ mice in parentheses): brain, 102 ± 7 (67 ± 9, mean ± SEM, values reported as PAR (peak area ratio in relation to stable-isotope labeled internal standard); liver, 156 ± 12 (95 ± 14) (Fig. 3A; $p<0.01$ for both brain and liver, two-tailed *t* test). We next examined the level of total GSH in RBCs derived from patients with SSADHD (n=9) and control individuals (n=7, composed of parents of patients, unaffected siblings, and unrelated control individuals, mixed gender and not age-matched). Total GSH was 330 ± 13 nmol/ml packed RBC (red blood cells) for control individuals (mean ± SEM) and 273 ± 22 for SSADHD patients ($p<0.05$, two tailed *t* test with Welch's correction) (Fig. 3B).

3.3 Quantitation of 4-HNE adducts in brain and liver of *aldh5a1*$^{-/-}$ and *aldh5a1*$^{+/+}$ mice

Because ALDH5A1 is the major aldehyde dehydrogenase responsible for further metabolism of 4-HNE [22], we tested the hypothesis that adducts of this reactive aldehyde intermediate would be elevated in brain and liver of *aldh5a1*$^{-/-}$ mice. Free 4-HNE is a very short-lived species, and its three reactive sites make it a target for adduction of various species (e.g., GSH). For 4-HNE adducts, we found in brain of *aldh5a1*$^{+/+}$ mice 33.6 ± 1.8 ug/mg protein (n=8 mice, mean ± SEM, mixed gender) and in *aldh5a1*$^{-/-}$ mice 48.1 ± 6.2 ($p<0.05$, two tailed *t* test) (Fig. 3C). These values in liver extracts were 30.5 ± 0.7 for *aldh5a1*$^{+/+}$ and 39.5 ± 5.7 for *aldh5a1*$^{-/-}$ mice (p=ns, two tailed *t* test).

3.4 Gene expression (mRNA) profiling

Based on earlier studies of the effect of rapamycin on mTOR signaling and biomarkers of oxidative stress in *aldh5a1*$^{-/-}$ mice [1], we next investigated the patterns of gene expression at the mRNA level for both *aldh5a1*$^{+/+}$ and *aldh5a1*$^{-/-}$ mice, with a focus on genes involved in mTOR signaling and maintenance of the intracellular oxidation-reduction homeostasis. Further, we examined the capacity of newer generation drugs (Tor 1, Tor 2) that inhibit mTOR signaling to improve mRNA levels corresponding to these genes (Tables 1, 2). Additional rationale for examining the molecular aspects (mRNA levels) related to Tor 1 and Tor 2 intervention in *aldh5a1*$^{-/-}$ mice derived from our finding that these agents are capable of significantly extending the lifespan of these mice [32].

3.4.1. mTOR-related gene expression (mRNA) profiles (Table 1)—In liver, the direction of expression of mRNA was decrease in untreated *aldh5a1*$^{-/-}$ mice for 13 of 20 genes quantified, as opposed to increase of mRNA levels for 7 genes. Either Tor 1 and Tor 2

resulted in the normalization (not significantly different from *aldh5a1*$^{+/+}$ mice) of mRNA levels for *Akt1a1, Ddit4, Eif4e and Rps6ka1* (Table 1). The application of Tor 2 resulted in the normalization of mRNA levels in *aldh5a1*$^{-/-}$ mice for *Pten, Rhoa, Rraga, Sgk1 and Tsc 1* (see Table 1 for quantitation of mRNA levels). Overall, the use of Tor 1 and 2 was associated with normalization of mRNA levels in *aldh5a1*$^{-/-}$ mice for 50% of genes (10/20) which showed dysregulated mRNA levels in *aldh5a1*$^{-/-}$ mice (untreated) compared to *aldh5a1*$^{+/+}$ mice. Conversely, looking at the mRNA level of mTOR-associated genes in the brain (23 total genes), results were less impressive than results in liver. In brain, the direction of mRNA level was decrease in untreated *aldh5a1*$^{-/-}$ mice for 13 of 23 genes quantified, as opposed to increase of mRNA level for 10 genes (data not shown). Only the mRNA level of *Akt1s1* in *aldh5a1*$^{-/-}$ mice was normalized to levels not significantly different from *aldh5a1*$^{+/+}$ mice by treatment with Tor 2 (data not shown). A schematic diagram of the relationship of the majority of these genes (Table 1), and their relationship to mTOR signaling, is shown in Fig. 4.

3.4.2. mRNA levels for genes associated with oxidative stress—We next turned attention to profiling of mRNA levels in *adlh5a1*$^{+/+}$ and *aldh5a1*$^{-/-}$ mice, and for the latter those that had been rescued from premature lethality with Tor 1 and 2, that focused on oxidative stress and/or maintenance of the intracellular redox potential in liver. This followed on our earlier work in which we had seen normalization of superoxide dismutase protein levels, and enzyme activity, in the liver of *aldh5a1*$^{-/-}$ mice treated with rapamycin [1]. In terms of mRNA levels reflecting expression of genes indicative of oxidative stress (Table 2), the level of mRNA in untreated *aldh5a1*$^{-/-}$ mice was a decrease in *Akr1c18, Aldh1a1, Casp3, Snca*, as opposed to increase in mRNA levels for *Ddit3* and *Dusp1)* (Table 2). Treatment of *aldh5a1*$^{-/-}$ mice with Tor 1 normalized the mRNA levels for *Dusp1* to a level indistinguishable from levels in *aldh5a1*$^{+/+}$ mice. Conversely, treatment of *aldh5a1*$^{-/-}$ mice with Tor 2 resulted in the normalization of mRNA levels for *Aldh1a1, Casp3,* and *Ddit3* to levels not significantly different from *aldh5a1*$^{+/+}$ mice. The mRNA levels for genes representing antioxidant enzymes in the liver was somewhat different, revealing that the direction of mRNA level for the 15 measured genes was almost uniformly decrease in untreated *aldh5a1*$^{-/-}$ mice as compared to *aldh5a1*$^{+/+}$ mice (Table 2; 14/15 genes overall). Intervention in *aldh5a1*$^{-/-}$ mice with either Tor 1 and Tor 2 resulted in mRNA levels of *Sod1 and Prdx2* that were indistinguishable from those observed for *aldh5a1*$^{+/+}$ mice. Intervention in *aldh5a1*$^{-/-}$ mice with Tor 2, however, resulted in mRNA levels for *Cat, Sod3, Gpx3, and Prdx6* (Table 2) to levels that were not significantly different from the levels observed in *aldh5a1*$^{+/+}$ mice.

3.5 Western blot analysis of selected proteins in *aldh5a1*$^{-/-}$ and *aldh5a1*$^{+/+}$ mice

To verify the results of gene expression analyses, we undertook immunoblot analysis of selected proteins in liver of *aldh5a1*$^{-/-}$ mice at two ages, DOL 11 and DOL 20 (Fig. 5). At both ages, *aldh5a1*$^{-/-}$ mice demonstrated a significant decrease of GSTT1 (glutathione transferase theta 1 subunit; Fig. 5B, 5F), consistent with down-regulated levels of mRNA (Table 2). Similar results were observed for the dimeric form of PRDX 1 (peroxiredoxin 1; Fig. 5D) which is the active form of the protein, accompanied by an increased concentration in DOL 20 *aldh5a1*$^{-/-}$ mice of the inactive monomeric form (Fig. 5H) [33]. SOD2

(superoxide dismutase 2, mitochondrial located) was elevated in *aldh5a1*$^{-/-}$ mice at both ages, although only significantly at DOL 11 (Fig. 5C, 5G). This is consistent with earlier work showing increased SOD2 enzyme activity in this mouse model, and reflects the elevated mitochondrial number in these mice which was previously improved with rapamycin [1]. Since *aldh5a1* is ablated in these animals, we explored several additional aldehyde dehydrogenase isoforms (*aldh1a1, aldh2, aldh 3a1, aldh4a, aldh6a1, aldh7a1 and aldh9a1*), in order to explore potential compensation in the mouse model for loss of *aldh5a1*. We found decreased levels of the *3a1* species and increased amounts of the *6a1* species (Fig. 5A, 5C). Of interest, *aldh3a1* has been suggested to promote resistance to 4-HNE-induced oxidative damage in the cornea, and lowered levels of this protein may add to the level of oxidative stress in *aldh5a1*$^{-/-}$ mice [34]. *Aldh6a1* encodes methylmalonate semialdehyde dehydrogenase, an enzyme on the valine catabolic pathway, with mitochondrial location [35, 36]. The mitochondrial location of this protein, and its elevated levels, is consistent with data on SOD2 in relation to increased mitochondrial numbers in *aldh5a1*$^{-/-}$ mice [1].

4. Discussion

The current report extends our characterization of mTOR inhibitors as a therapeutic consideration for SSADHD. We present the first comprehensive analyses of GABA, GHB, D-2-HG, SSA, and DHHA (Fig. 2A–2E) in multiple tissues, also demonstrating for the first time a significant increase of SSA in peripheral tissues of *aldh5a1*$^{-/-}$ mice [16, 27, 29, 37]. The majority of these metabolites induce oxidative stress when administered individually to rodents [16–20], which formed the rationale underlying our gene expression analysis targeting the cellular oxidation-reduction potential. The data of Fig. 2 suggests that the metabolic equilibrium in *aldh5a1*$^{-/-}$ mice favors GHB production from SSA by ~25–30-fold. Why SSA levels would be present in *aldh5a1*$^{+/+}$ mice, in view of the low K_m of SSADH (~1–4 μM) [38] for SSA, is not readily explained. The presence of SSA in *aldh5a1*$^{+/+}$ might relate to the “dynamic catalytic loop” of the SSADH protein which is susceptible to oxidative stress conditions and subsequent inactivation [39–41], suggesting that some level of SSA might always be present. Of interest, a recent report has demonstrated that *aldh1a1* mediates a GABA synthesis pathway in midbrain dopaminergic neurons [42]. The finding of significantly decreased mRNA encoding *aldh1a1* (Table 2) could potentially help to explain the increased levels of SSA in *aldh5a1*$^{-/-}$ mice (combined with loss of *aldh5a1*), but does not readily shed light on the accumulation of SSA in *aldh5a1*$^{+/+}$ mice.

The data of Fig. 3 verify global disruptions of the cellular oxidation-reduction potential in *aldh5a1*$^{-/-}$ mice, and we verify for the first time that total glutathione is significantly depleted in multiple patients with SSADHD, and 4-HNE adducts are significantly increased in the liver of *aldh5a1*$^{-/-}$ mice. Our rationale for evaluation of 4-HNE adducts centered on our earlier work verifying that SSADH is the major enzyme involved in 4-HNE metabolism in brain [22], but not in liver, and the prediction with the loss of SSADH activity in *aldh5a1*$^{-/-}$ mice that 4-HNE, and correspondingly 4-HNE adducts, would be increased. Increased levels of 4-HNE in the brain of *aldh5a1*$^{-/-}$ mice, and by extrapolation to the brain of patients with SSADHD, might correlate with the clinical picture of patients, in which neuroimaging reveals hyperintensities of the basal ganglia [2]. These hyperintensities may

well relate to oxidative stress [43]. Armed with the preceding metabolic evidence for oxidative stress in *aldh5a1*$^{-/-}$ mice, we opted to pursue a global assessment of both mTOR signaling and oxidative stress employing gene expression analysis for mRNA levels. Our rationale for these studies centered on earlier work with GABA, mTOR and oxidative stress [1, 13, 32], in which we showed that elevated GABA, acting via mTOR, induced accumulation of mitochondria and enhanced oxidative stress. The finding that rapamycin could mitigate these effects led us to investigate newer generation mTOR inhibitors. We chose to utilize Torin 1 in lieu of rapamycin because Torin 1 is highly potent and selective, and several mTORC1 (mechanistic target of rapamycin complex 1) functions are resistant to inhibition by rapamycin, yet effectively blocked by the newer analog Torin 1 [44, 45]. Torin 2 is a novel, second-generation ATP-competitive inhibitor that is potent and selective for mTOR with a superior pharmacokinetic profile to previous inhibitors, including Torin 1 [46]. Accordingly, we evaluated the treatment of *aldh5a1*$^{-/-}$ mice with both compounds, followed by subsequent studies of mRNA levels.

The data of Table 1, focused on mRNA levels in *aldh5a1*$^{-/-}$ mice in the presence and absence of mTOR inhibitors, provide further evidence for abnormal PI3K/AKT/mTOR signaling (Fig. 4). Concentrations of mRNA encoding effectors of this signaling pathway were clearly dysregulated in untreated *aldh5a1*$^{-/-}$ mice, including decreased levels of mRNA encoding *Ulk2* and *Elf4e*, and increased mRNA levels encoding *Rps6ka1* (Table 1). These expression anomalies were not induced by a corresponding increase in mRNA levels for insulin-like growth factor (*Igf-1*), whose mRNA levels were actually decreased in *ald5a1*$^{-/-}$ mice. The relationships between IGF-1 and mTOR signaling has been well established [47]. Consistent with our finding of low *Igf-1* mRNA in *aldh5a1*$^{-/-}$ mice was the demonstration of low *Igf1* levels in blood from a patient with GABA-transaminase deficiency [48], a disorder also accompanied by elevated GABA in tissues and body fluids. Autocrine GABA (working via activation of $GABA_A$ receptors) can depolarize pancreatic β-cells and enhance insulin secretion, and insulin can down-regulate $GABA_A$-ergic signaling as a feedback mechanism for fine-tuning of insulin secretion [49, 50]. Importantly, mRNA levels encoding *Sgk1* were increased in untreated *aldh5a1*$^{-/-}$ mice, and *Sgk1* is a gene whose activity is induced by both PI3K and mTORC2. Dysregulation of the mRNA levels encoding *Sgk1* has been associated with oxidative stress, as well as dopamine maintenance and epilepsy, all of which form components of the underlying SSADHD phenotype.

Previous work from our lab and others adds further support to the probable relationship between elevated GABA and altered mTOR expression seen in Table 1. Along those lines, the data of Lakhani and coworkers (2014) verified that increased mTOR signaling, as measured using phosphoS6 kinase analysis, could be significantly attenuated with the mTOR inhibitor rapamycin. These studies were performed both in brain and liver, which verified a more systemic correction that lends further support to our expression array data. Additionally, inhibition of mTOR leads to mRNA degradation of selected species, and has no effect of other species, in brain while mTOR still regulates the translation of selected mRNAs [51]. These observations may underscore why we saw limited (if any) correction of expression analyses in the brain of *aldh5a1*$^{-/-}$ as opposed to the significant corrections observed in liver.

Turning attention to Table 2 and mRNA levels associated with oxidative stress, previous studies in *aldh5a1*$^{-/-}$ mice have shown that total radical-trapping antioxidant potential was significantly decreased in liver and cerebral cortex, SOD (superoxide dismutase) activity was elevated in liver and cerebellum, and catalase activity (a quencher of peroxisomal hydroxyl radicals) was elevated in thalamus [17, 18]. Additionally, glutathione peroxidase was decreased in hippocampus, and thiobarbaturic acid-reactive species (TBARS; indicative of lipid peroxidation) were markedly elevated in liver and cerebral cortex of *aldh5a1*$^{-/-}$ mice. The data of Table 2, highlighting decreased levels of mRNA encoding catalase, superoxide dismutase, glutathione peroxidase and glutathione transferase in untreated *aldh5a1*$^{-/-}$ mice, are consistent with the previously published enzyme studies in tissues, and have been further corroborated in the current study using Western blot analyses (Fig. 5). Further, Table 2 revealed alterations in the mRNA levels in *aldh5a1*$^{-/-}$ mice that encode peroxiredoxins, a family of antioxidant enzymes that also control cytokine-induced peroxide levels and thereby mediate signal transduction in mammalian cells [52]. Additionally, we observed a significant decrease in the level of mRNA encoding *aldh1a1* in the liver of *aldh5a1*$^{-/-}$ mice that was returned to levels that were not significantly different from *aldh5a1*$^{+/+}$ mice using Tor 2 (Table 2)

5. Conclusions

We provide metabolic, protein and molecular genetic data supporting the concept that inhibition of mTOR has therapeutic relevance in *aldh5a1*$^{-/-}$ mice, and by extension, patients with SSADHD.

Acknowledgments

This work was supported by R21 NS 85369. We thank the patients with SSADHD who donated blood samples, and the SSADH Association for their continued support.

References

1. Lakhani R, Vogel KR, Till A, Liu J, Burnett SF, Gibson KM, Subramani S. Defects in GABA metabolism affect selective autophagy pathways and are alleviated by mTOR inhibition. EMBO Mol Med. 2014; 6:551–566. DOI: 10.1002/emmm.201303356 [PubMed: 24578415]
2. Lapalme-Remis S, Lewis EC, De Meulemeester C, Chakraborty P, Gibson KM, Torres C, Guberman A, Salomons GS, Jakobs C, Ali-Ridha A, Parviz M, Pearl PL. Natural history of succinic semialdehyde dehydrogenase deficiency through adulthood. Neurology. 2015; doi: 10.1212/WNL.0000000000001906
3. Pearl, PL.; Koenig, M.; Riviello, J.; Christie, JM.; Averill, K.; Chung, W.; Bain, J.; Chiriboga, C.; Hodgeman, R.; Parviz, M.; Gibson, K. Novel intervention in GABA-transaminase deficiency. Child Neurol. Soc, Annual Meeting; 2015. in press
4. Rodan LH, Gibson KM, Pearl PL. Clinical Use of CSF Neurotransmitters. Pediatr Neurol. 2015; 53:277–286. DOI: 10.1016/j.pediatrneurol.2015.04.016 [PubMed: 26194033]
5. Parviz M, Vogel K, Gibson KM, Pearl PL. Disorders of GABA metabolism: SSADH and GABA-transaminase deficiencies. J Pediatr Epilepsy. 2014; 3:217–227. DOI: 10.3233/PEP-14097 [PubMed: 25485164]
6. Pearl PL, Parviz M, Vogel K, Schreiber J, Theodore WH, Gibson KM. Inherited disorders of gamma-aminobutyric acid metabolism and advances in ALDH5A1 mutation identification. Dev Med Child Neurol. 2014; doi: 10.1111/dmcn.12668

7. Snead OC, Gibson KM. Gamma-hydroxybutyric acid. N Engl J Med. 2005; 352:2721–2732. DOI: 10.1056/NEJMra044047 [PubMed: 15987921]

8. Maitre M, Klein C, Mensah-Nyagan AG. Mechanisms for the Specific Properties of γ-Hydroxybutyrate in Brain. Med Res Rev. 2016; doi: 10.1002/med.21382

9. Dósa Z, Nieto-Gonzalez JL, Korshoej AR, Gibson KM, Jensen K. Effect of gene dosage on single-cell hippocampal electrophysiology in a murine model of SSADH deficiency (gamma-hydroxybutyric aciduria). Epilepsy Res. 2010 Jun; 90(1–2):39–46. Epub 2010 Apr 3. DOI: 10.1016/j.eplepsyres.2010.03.005 [PubMed: 20363598]

10. Hogema BM, Gupta M, Senephansiri H, Burlingame TG, Taylor M, Jakobs C, Schutgens RBH, Froestl W, Snead OC, Diaz-Arrastia R, Bottiglieri T, Grompe M, Gibson KM. Pharmacologic rescue of lethal seizures in mice deficient in succinate semialdehyde dehydrogenase. Nat Genet. 2001; 29:212–216. DOI: 10.1038/ng727 [PubMed: 11544478]

11. Vogel KR, Pearl PL, Theodore WH, McCarter RC, Jakobs C, Gibson KM. Thirty years beyond discovery-Clinical trials in succinic semialdehyde dehydrogenase deficiency, a disorder of GABA metabolism. J Inherit Metab Dis. 2013; 36:401–410. [PubMed: 22739941]

12. Vardya I, Drasbek KR, Gibson KM, Jensen K. Plasticity of postsynaptic, but not presynaptic, GABAB receptors in SSADH deficient mice. Exp Neurol. 2010 Sep; 225(1):114–22. Epub 2010 Jun 4. DOI: 10.1016/j.expneurol.2010.05.022 [PubMed: 20570675]

13. Vogel KR, Ainslie GR, Jansen EEW, Salomons GS, Gibson KM. Torin 1 partially corrects vigabatrin-induced mitochondrial increase in mouse. Ann Clin Transl Neurol. 2015; 2:699–706. DOI: 10.1002/acn3.200 [PubMed: 26125044]

14. Weston MC, Chen H, Swann JW. Multiple roles for mammalian target of rapamycin signaling in both glutamatergic and GABAergic synaptic transmission. J Neurosci Off J Soc Neurosci. 2012; 32:11441–11452. DOI: 10.1523/JNEUROSCI.1283-12.2012

15. Workman ER, Niere F, Raab-Graham KF. mTORC1-dependent protein synthesis underlying rapid antidepressant effect requires GABABR signaling. Neuropharmacology. 2013; 73:192–203. DOI: 10.1016/j.neuropharm.2013.05.037 [PubMed: 23752093]

16. Gibson, KM.; Gupta, M.; Senephansiri, H.; Jansen, EEW.; Montine, TJ.; Hyland, K.; Switzer, RC.; Snead, OC.; Jakobs, C. Oxidant stress and neurodegeneration in murine succinic semialdehyde dehydrogenase (SSADH) deficiency. In: Hoffmann, GF., editor. Diseases of Neurotransmission-from bench to bed. SPS Verlagsgessellschaft mbH; Heilbronn, Germany: 2006. p. 199-212.Symposia Proceedings

17. Latini A, Scussiato K, Leipnitz G, Gibson KM, Wajner M. Evidence for oxidative stress in tissues derived from succinate semialdehyde dehydrogenase-deficient mice. J Inherit Metab Dis. 2007; 30:800–810. DOI: 10.1007/s10545-007-0599-6 [PubMed: 17885820]

18. Sauer SW, Kölker S, Hoffmann GF, Ten Brink HJ, Jakobs C, Gibson KM, Okun JG. Enzymatic and metabolic evidence for a region specific mitochondrial dysfunction in brains of murine succinic semialdehyde dehydrogenase deficiency (Aldh5a1−/− mice). Neurochem Int. 2007; 50:653–659. DOI: 10.1016/j.neuint.2006.12.009 [PubMed: 17303287]

19. Sgaravatti AM, Sgarbi MB, Testa CG, et al. Gamma-hydroxybutyric acid induces oxidative stress in cerebral cortex of young rats. Neurochem Int. 2007; 50:564–70. [PubMed: 17197055]

20. da Rosa MS, Seminotti B, Amaral AU, Parmeggiani B, de Oliveira FH, Leipnitz G, Wajner M. Disruption of redox homeostasis and histopathological alterations caused by in vivo intrastriatal administration of D-2-hydroxyglutaric acid to young rats. Neuroscience. 2014 Sep 26.277:281–93. Epub 2014 Jul 17. DOI: 10.1016/j.neuroscience.2014.07.011 [PubMed: 25043325]

21. Niemi A-K, Brown C, Moore T, Enns GM, Cowan TM. Low glutathione levels in a patient with succinic semialdehyde dehydrogenase (SSADH) deficiency. Molec Genet Metab. 2012; 105:345. (abstract).

22. Murphy TC, Amarnath V, Gibson KM, Picklo MJ Sr. Oxidation of 4-hydroxy-2-nonenal by succinic semialdehyde dehydrogenase (ALDH5A). J Neurochem. 2003 Jul; 86(2):298–305. [PubMed: 12871571]

23. Gibson, KM.; Aramaki, S.; Sweetman, L.; Nyhan, WL.; DeVivo, DC.; Hodson, AK.; Jakobs, C. Stable isotope dilution analysis of 4-hydroxybutyric acid: an accurate method for quantification in

physiological fluids and the prenatal diagnosis of 4-hydroxybutyric aciduria. Biomed. Environ. Mass Spectrom; 1990; p. 89-93.

24. Kok RM, Howells DW, van den Heuvel CC, Guérand WS, Thompson GN, Jakobs C. Stable isotope dilution analysis of GABA in CSF using simple solvent extraction and electron-capture negative-ion mass fragmentography. J Inherit Metab Dis. 1993; 16:508–512. [PubMed: 7541876]
25. Struys EA, Jansen EEW, Gibson KM, Jakobs C. Determination of the GABA analogue succinic semialdehyde in urine and cerebrospinal fluid by dinitrophenylhydrazine derivatization and liquid chromatography-tandem mass spectrometry: application to SSADH deficiency. J Inherit Metab Dis. 2005; 28:913–920. DOI: 10.1007/s10545-005-0111-0 [PubMed: 16435183]
26. Struys EA, Jansen EE, Verhoeven NM, Jakobs C. Measurement of urinary D- and L-2-hydroxyglutarate enantiomers by stable-isotope-diluation liquid chromatography-tandem mass spectrometry after derivatization with diacetyl-L-tartaric anhydride. Clin Chem. 2004; 50:1391–1395. DOI: 10.1373/clinchem.2004.033399 [PubMed: 15166110]
27. Struys EA, Verhoeven NM, Jansen EEW, Ten Brink HJ, Gupta M, Burlingame TG, Quang LS, Maher T, Rinaldo P, Snead OC, Goodwin AK, Weerts EM, Brown PR, Murphy TC, Picklo MJ, Jakobs C, Gibson KM. Metabolism of gamma-hydroxybutyrate to d-2-hydroxyglutarate in mammals: further evidence for d-2-hydroxyglutarate transhydrogenase. Metabolism. 2006; 55:353–358. DOI: 10.1016/j.metabol.2005.09.009 [PubMed: 16483879]
28. Moore ME, Loft JM, Clegern WC, Wisor JP. Manipulating neuronal activity in the mouse brain with ultrasound: A comparison with optogenetic activation of the cerebral cortex. Neurosci Lett. 2015; 604:183–187. DOI: 10.1016/j.neulet.2015.07.024 [PubMed: 26222259]
29. Gupta M, Greven R, Jansen EEW, Jakobs C, Hogema BM, Froestl W, Snead OC, Bartels H, Grompe M, Gibson KM. Therapeutic intervention in mice deficient for succinate semialdehyde dehydrogenase (gamma-hydroxybutyric aciduria). J Pharmacol Exp Ther. 2002; 302:180–187. [PubMed: 12065715]
30. Bustin SA, Benes V, Garson JA, Hellemans J, Huggett J, Kubista M, Mueller R, Nolan T, Pfaffl MW, Shipley GL, Vandesompele J, Wittwer CT. The MIQE guidelines: minimum information for publication of quantitative real-time PCR experiments. Clin Chem. 2009; 55:611–622. DOI: 10.1373/clinchem.2008.112797 [PubMed: 19246619]
31. Yuan JS, Reed A, Chen F, Stewart CN Jr. Statistical analysis of real-time PCR data. BMC Bioinformatics. 2006 Feb 22.7:85. [PubMed: 16504059]
32. Vogel KE, Ainslie GR, Gibson KM. mTOR Inhibitors Rescue Premature Lethality and Attenuate Dysregulation of GABAergic/Glutamatergic Transcription in Murine Succinate Semialdehyde Dehydrogenase Deficiency (SSADHD), a Disorder of GABA Metabolism. J Inherited Metab Dis. in press.
33. Huang CY1, Chen YT, Wen L, Sheu DC, Lin CT. A peroxiredoxin cDNA from Taiwanofungus camphorata: role of Cys31 in dimerization. Mol Biol Rep. 2014 Jan; 41(1):155–64. Epub 2013 Nov 6. DOI: 10.1007/s11033-013-2848-0 [PubMed: 24194195]
34. Black W, Chen Y, Matsumoto A, Thompson DC, Lassen N, Pappa A, Vasiliou V. Molecular mechanisms of ALDH3A1-mediated cellular protection against 4-hydroxy-2-nonenal. Free Radic Biol Med. 2012 May 1; 52(9):1937–44. Epub 2012 Mar 8. DOI: 10.1016/j.freeradbiomed.2012.02.050 [PubMed: 22406320]
35. Sass JO, Walter M, Shield JP, Atherton AM, Garg U, Scott D, Woods CG, Smith LD. 3-Hydroxyisobutyrate aciduria and mutations in the ALDH6A1 gene coding for methylmalonate semialdehyde dehydrogenase. J Inherit Metab Dis. 2012 May; 35(3):437–42. Epub 2011 Aug 24. DOI: 10.1007/s10545-011-9381-x [PubMed: 21863277]
36. Chambliss KL, Gray RG, Rylance G, Pollitt RJ, Gibson KM. Molecular characterization of methylmalonate semialdehyde dehydrogenase deficiency. J Inherit Metab Dis. 2000 Jul; 23(5):497–504. [PubMed: 10947204]
37. Gibson KM, Schor DSM, Gupta M, Guerand WS, Senephansiri H, Burlingame TG, Bartels H, Hogema BM, Bottiglieri T, Froestl W, Snead OC, Grompe M, Jakobs C. Focal neurometabolic alterations in mice deficient for succinate semialdehyde dehydrogenase. J Neurochem. 2002; 81:71–79. [PubMed: 12067239]

38. Chambliss KL, Gibson KM. Succinic semialdehyde dehydrogenase from mammalian brain: subunit analysis using polyclonal antiserum. Int J Biochem. 1992 Sep; 24(9):1493–9. [PubMed: 1426531]
39. Kim Y-G, Lee S, Kwon O-S, Park S-Y, Lee S-J, Park B-J, Kim K-J. Redox-switch modulation of human SSADH by dynamic catalytic loop. EMBO J. 2009; 28:959–968. DOI: 10.1038/emboj.2009.40 [PubMed: 19300440]
40. Kim K-J, Pearl PL, Jensen K, Snead OC, Malaspina P, Jakobs C, Gibson KM. Succinic semialdehyde dehydrogenase: biochemical-molecular-clinical disease mechanisms, redox regulation, and functional significance. Antioxid Redox Signal. 2011; 15:691–718. DOI: 10.1089/ars.2010.3470 [PubMed: 20973619]
41. Tamazian G, Ho Chang J, Knyazev S, Stepanov E, Kim KJ, Porozov Y. Modeling conformational redox-switch modulation of human succinic semialdehyde dehydrogenase. Proteins. 2015; 83:2217–2229. DOI: 10.1002/prot.24937 [PubMed: 26422261]
42. Kim JI, Ganesan S, Luo SX, Wu YW, Park E, Huang EJ, Chen L, Ding JB. Aldehyde dehydrogenase 1a1 mediates a GABA synthesis pathway in midbrain dopaminergic neurons. Science. 2015; 350:102–106. DOI: 10.1126/science.aac4690 [PubMed: 26430123]
43. Bartzokis G, Tishler TA, Lu PH, Villablanca P, Altshuler LL, Carter M, Huang D, Edwards N, Mintz J. Brain ferritin iron may influence age- and gender-related risks of neurodegeneration. Neurobiol Aging. 2007 Mar; 28(3):414–23. Epub 2006 Mar 24. [PubMed: 16563566]
44. Thoreen CC, Kang SA, Chang JW, Liu Q, Zhang J, Gao Y, Reichling LJ, Sim T, Sabatini DM, Gray NS. An ATP-competitive mammalian target of rapamycin inhibitor reveals rapamycin-resistant functions of mTORC1. J Biol Chem. 2009 Mar 20; 284(12):8023–32. Epub 2009 Jan 15. DOI: 10.1074/jbc.M900301200 [PubMed: 19150980]
45. Lamming DW, Ye L, Sabatini DM, Baur JA. Rapalogs and mTOR inhibitors as anti-aging therapeutics. J Clin Invest. 2013 Mar; 123(3):980–9. Epub 2013 Mar 1. Review. DOI: 10.1172/JCI64099 [PubMed: 23454761]
46. Simioni C, Cani A, Martelli AM, Zauli G, Tabellini G, McCubrey J, Capitani S, Neri LM. Activity of the novel mTOR inhibitor Torin-2 in B-precursor acute lymphoblastic leukemia and its therapeutic potential to prevent Akt reactivation. Oncotarget. 2014 Oct 30; 5(20):10034–47. [PubMed: 25296981]
47. Damerill I, Biggar KK, Abu Shehab M, Li SSC, Jansson T, Gupta MB. Hypoxia Increases IGFBP-1 Phosphorylation Mediated by mTOR Inhibition. Mol Endocrinol Baltim Md. 2016; 30:201–216. DOI: 10.1210/me.2015-1194
48. Tsuji M, Aida N, Obata T, Tomiyasu M, Furuya N, Kurosawa K, Errami A, Gibson KM, Salomons GS, Jakobs C, Osaka H. A new case of GABA transaminase deficiency facilitated by proton MR spectroscopy. J Inherit Metab Dis. 2010; 33:85–90. DOI: 10.1007/s10545-009-9022-9 [PubMed: 20052547]
49. Bansal P, Wang S, Liu S, Xiang YY, Lu WY, Wang Q. GABA coordinates with insulin in regulating secretory function in pancreatic INS-1 β-cells. PloS One. 2011; 6:e26225.doi: 10.1371/journal.pone.0026225 [PubMed: 22031825]
50. Soltani N, Qiu H, Aleksic M, Glinka Y, Zhao F, Liu R, Li Y, Zhang N, Chakrabarti R, Ng T, Jin T, Zhang H, Lu W-Y, Feng Z-P, Prud'homme GJ, Wang Q. GABA exerts protective and regenerative effects on islet beta cells and reverses diabetes. Proc Natl Acad Sci U S A. 2011; 108:11692–11697. DOI: 10.1073/pnas.1102715108 [PubMed: 21709230]
51. Sosanya NM, Huang PP, Cacheaux LP, Chen CJ, Nguyen K, Perrone-Bizzozero NI, Raab-Graham KF. Degradation of high affinity HuD targets releases Kv1.1 mRNA from miR-129 repression by mTORC1. J Cell Biol. 2013; 202(1):53–69. [PubMed: 23836929]
52. Rhee SG, Chae HZ, Kim K. Peroxiredoxins: a historical overview and speculative preview of novel mechanisms and emerging concepts in cell signaling. Free Radic Biol Med. 2005; 38:1543–1552. DOI: 10.1016/j.freeradbiomed.2005.02.026 [PubMed: 15917183]
53. Brown GK, Cromby CH, Manning NJ, Pollitt RJ. Urinary organic acids in succinic semialdehyde dehydrogenase deficiency: evidence of alpha-oxidation of 4-hydroxybutyric acid, interaction of succinic semialdehyde with pyruvate dehydrogenase and possible secondary inhibition of mitochondrial beta-oxidation. J Inherit Metab Dis. 1987; 10:367–375. [PubMed: 3126356]

Highlights

- Elevated GABA in *aldh5a1*$^{-/-}$ mice alters mTOR signaling and autophagy
- mTOR inhibition improves dysregulated mTOR signaling in *aldh5a1*$^{-/-}$ mice
- mTOR inhibition improves abnormalities of oxidative stress in *aldh5a1*$^{-/-}$ mice
- Outcomes in *adldh5a1*$^{-/-}$ mice were optimal with the mTOR inhibitor, Torin 2
- Torin 2 is therapeutically relevant in the GABA defect, SSADH deficiency

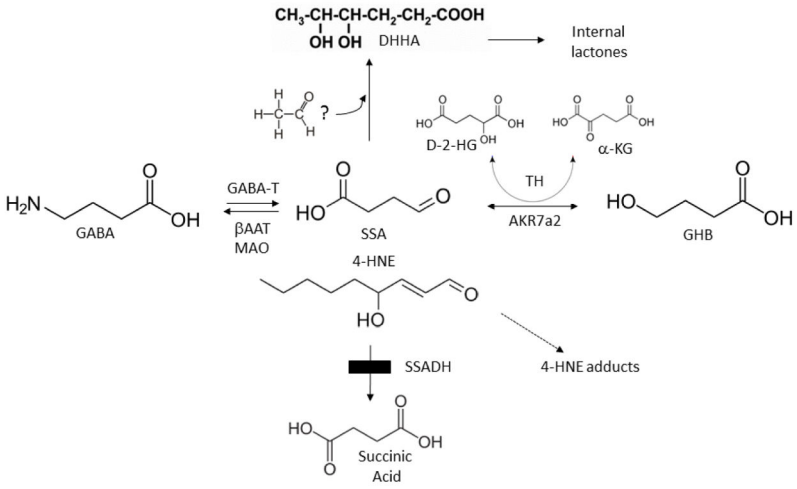

Fig. 1. Schematic diagram of GABA metabolism and metabolic abnormalities in *aldh5a1*$^{-/-}$ mice

4-Aminobutyric acid (also γ-aminobutyric acid; GABA) is normally metabolized to succinic semialdehyde via GABA-transaminase (GABA-T), and subsequently forms succinic acid via succinic semialdehyde dehydrogenase (SSADH), the defect in SSADH deficiency (SSADHD; box). Multiple metabolites are elevated in tissues of *aldh5a1*$^{-/-}$ mice, and in physiological fluids derived from patients with SSADHD. These include: γ-hydroxybutyrate (GHB; produced from succinic semialdehyde (SSA) in a reaction catalyzed by aldo-keto reductase 7a2, AKR7a2); D-2-hydroxyglutaric acid (D-2-HG; produced in a reaction catalyzed by nicotinamide-independent D-2-hydroxyglutaric transhydrogenase (TH), which stoichiometrically interconverts SSA and GHB coupled to the interconversion of D-2-HG with α-ketoglutarate (a-KG)), succinic semialdehyde (SSA); and 4,5-dihydroxyhexanoic acid (DHHA; no enzyme reaction has been identified that catalyzes the formation of DHHA, but it may be derived from SSA condensation with an “activated” two carbon species, perhaps within the pathway of oxidative phosphorylation [53]). In addition to GABA-T, monoamine oxidase (MAO) and β-alanine aminotransferase (βAAT) can also metabolize GABA. Also shown is 4-hydroxy-2-nonenal (4-HNE), which is metabolized to 4-HNE acid in brain in a reaction catalyzed by SSADH. Note the structural similarities of 4-HNE and SSA.

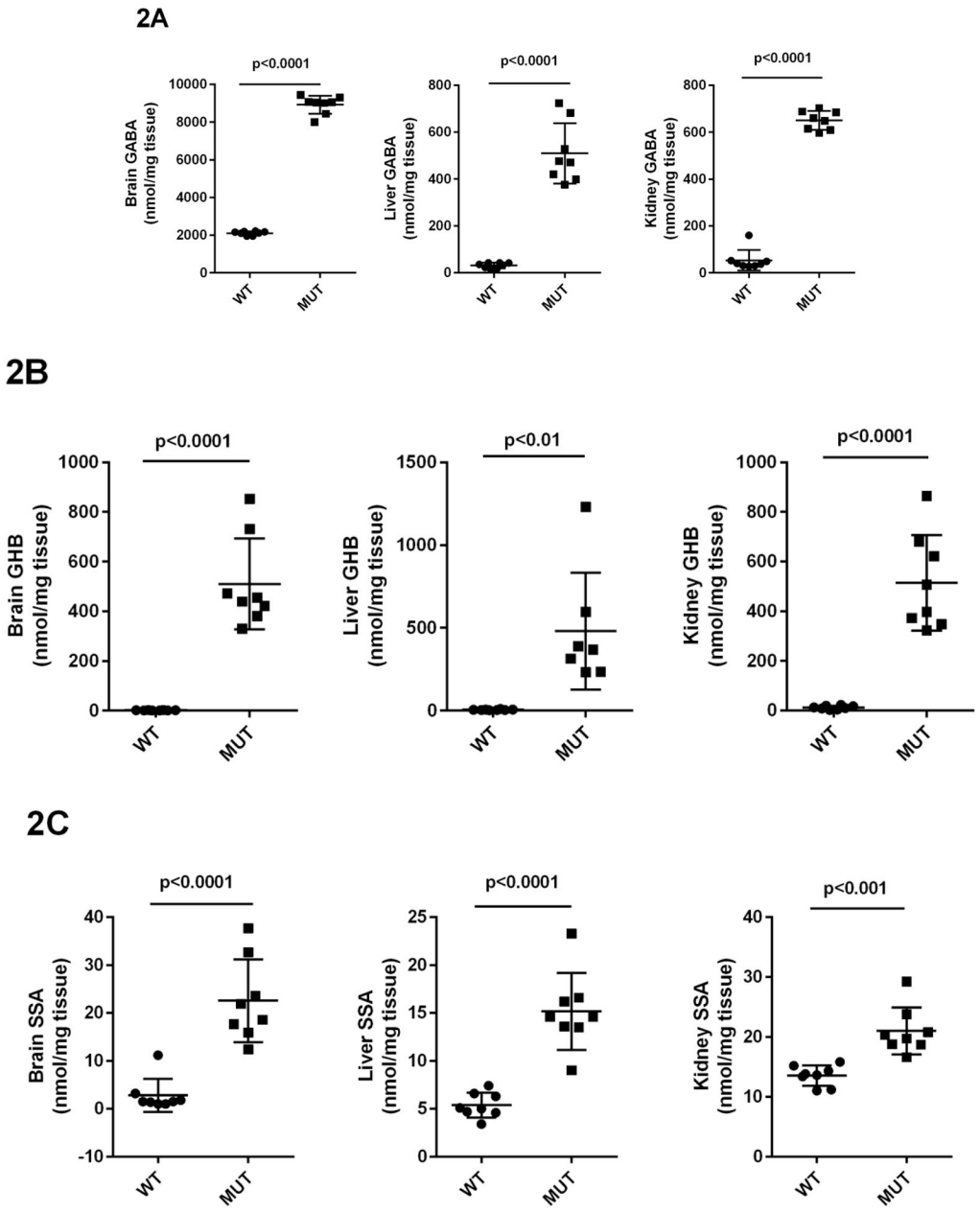

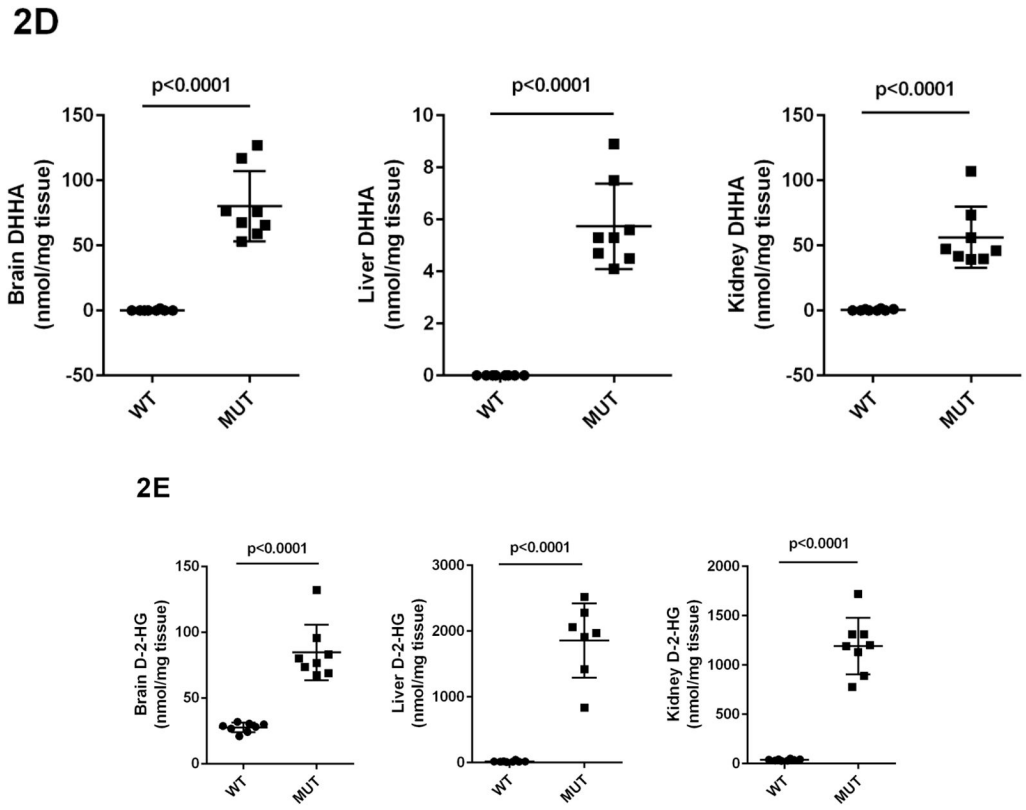

Fig 2A–2E. GABA and related metabolites in tissues derived from *aldh5a1*$^{+/+}$ (wild-type; WT, n=8) and *aldh5a1*$^{-/-}$ (mutant; MUT, n=8) mice

Metabolites include GABA (2A; γ-aminobutyric acid), GHB (2B; γ-hydroxybutyric acid), SSA (2C; succinic semialdehyde), DHHA (2D; 4,5-dihydroxyhexanoic acid) and D-2-HG (2E; D-2-hydroxyglutaric acid). Tissues surveyed included liver (L), kidney (K) and brain (B). Data depicted as mean ± SEM, with error bars indicating SEM and central horizontal bar indicating mean. Student's *t* test was used for statistical evaluation (two-tailed).

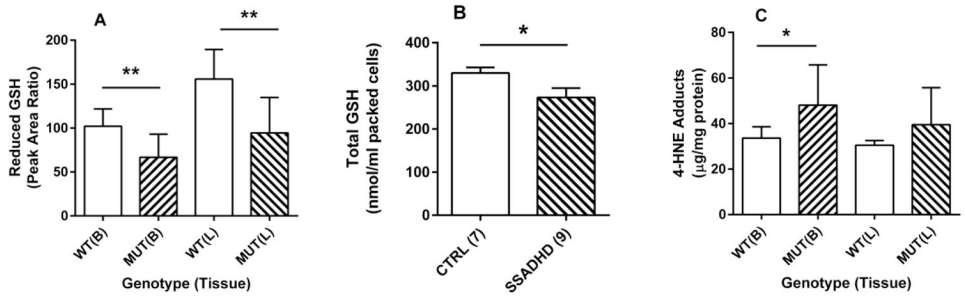

Fig. 3. Glutathione and 4-HNE adducts in extracts of brain and liver of *aldh5a1*$^{-/-}$ (mutant; MUT, n=8) and *aldh5a1*$^{+/+}$ (wild-type; WT, n=8) mice or red blood cells (RBCs) derived from patients with SSADHD

(A) Quantitation of reduced glutathione in *aldh5a1*$^{-/-}$ mice vs. *aldh5a1*$^{+/+}$ mice. (B) GSH (total) in SSADHD patient red blood cell extracts (CTR=control individuals; SSADHD, patients with SSADH deficiency). Parenthetical values denote the number of individuals studied (C) Adducts of 4-HNE in tissues of *aldh5a1*$^{+/+}$ and *aldh5a1*$^{-/-}$ mice. Data depicted as mean ± SEM. Statistical analyses employed a two-tailed *t* test (*p<0.05; **p<0.01).

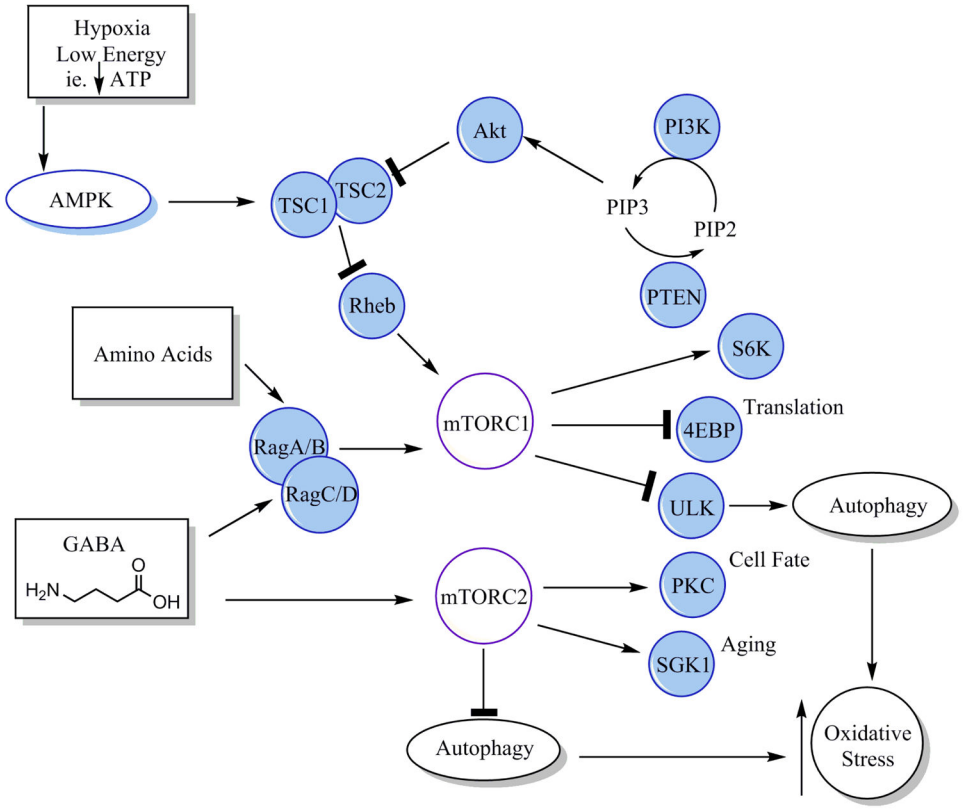

Fig. 4. Schematic diagram of mTOR signaling and proposed activation mechanisms by elevated GABA

This diagram is presented to provide guidance in the interpretation of the data of Table 1. Upstream activation of the mTOR complexes (mTORC1/mTORC2) can occur through tyrosine kinase receptors, insulin/Akt (protein kinase B), growth factors, and amino acids. AMPK (5′ AMP-activated protein kinase) modulates low energy status signals and inhibits mTOR through activation of TSC1/2 (tuberous sclerosis complexes). Additional abbreviations: Rheb, ras homolog enriched in brain; PI3K, phosphatidylinositol-4,5-bisphosphate 3-kinase; PIP3, phosphatidylinositol (3,4,5)-trisphosphate; PIP2, phosphatidylinositol 4,5-bisphosphate; PTEN, phosphate and tensin homolog; S6K, ribosomal protein S6 kinase; 4EBP, factor 4E binding protein; ULK, Unc-51 like autophagy activating kinase; PKC, protein kinase C; SGK1, serum and glucocorticoid-regulated kinase 1; Rag A-D, Ras-related GTP binding proteins A, B, C and D. Solid bars attached to lines indicate inhibition, wherease arrows indicate activation.

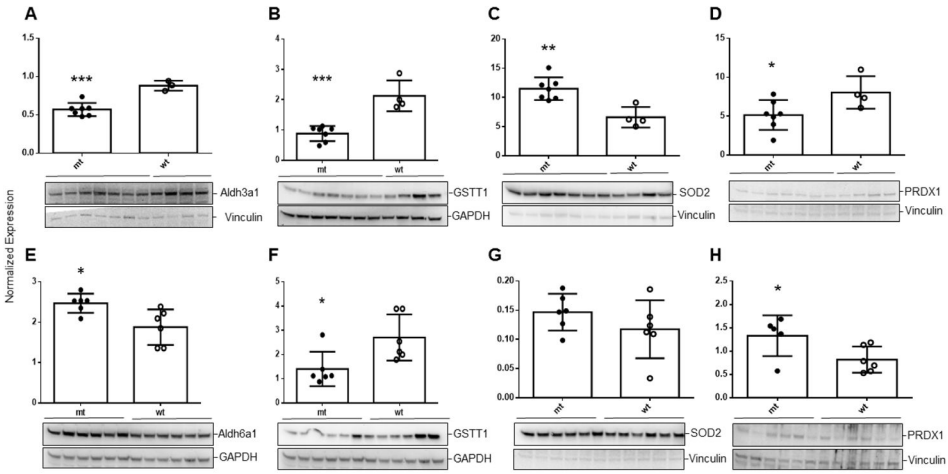

Fig. 5. Western blot analysis of selected proteins in liver extracts derived from *aldh5a1*$^{-/-}$ (mt) and *aldh5a1*$^{+/+}$ (wt) littermates

Immunoblot analyses are shown in each frame (A-H) below the normalized expression values (mean ± SD of normalized band intensities). Loading controls included either vinculin or GAPDH (glyceraldehyde-3-phosphate dehydrogenase). Horizontal bars below mouse genotype indicate the number of animals studied for each protein. Livers harvested from mice (DOL (day of life) 11) were interrogated for *aldh3a1* (A), glutathione S-transferase theta 1 subunit (GSTT1; B), superoxide dismutase 2 (SOD2 (mitochondrial)); and the dimer form of peroxiredoxin (PRDX1; D). Livers from animals harvested at DOL 20 were similarly examined for GSTT1, SOD2 and PRDX1 (F–H) as well as *aldh6a1* (E). Note that PRDX1 in H represents the monomer (inactive) form of the protein. Statistical analysis employed a two-tailed *t*-test where *p <0.05, **p<0.01, and ***p<0.001. mRNA levels for GSTT1, SOD2 and PRDX1 are also quantified in Table 2.

Table 1

mTOR pathway related expressional changes in liver.

Target	RNE/ Fold Change	P	Gene Name and Description of Activity
Akt1s1	1.74/1.74	0.0001	Akt1 substrate; subunit of mTORC1
	1.27/1.27	0.11	
	1.31/1.31	0.05	
Ddit4	4.28/4.28	0.0001	DNA damage inducible transcript 4; inhibits mTORC1
	1.22/1.22	0.08	
	0.87/−1.15	0.35	
Ddit4l	0.26/−3.81	0.02	See *Ddit4*: regulates mTOR upstream of TSC1-TSC2 and downstream of Akt1
	9.48/9.48	0.01	
	0.31/−3.27	0.02	
Eif4e	0.16/−6.24	0.04	Eukaryotic translation initiation factor 4E; related to PI3K/Akt signaling
	0.11/−8.80		
	0.49/−2.03	0.11	
Eif4ebp2	1.61/1.61	0.0001	See *Eif4e*; binding protein 2 which binds *Eif4e* to inhibit translation
	1.28/1.28	0.0001	
	2.00/2.00	0.0001	
Igf1	0.21/−4.87	0.01	Insulin-like growth factor
	0.29/−3.46	0.01	
	0.26/−3.78	0.01	
Pik3cb	4.04/4.04	0.10	Phosphatidylinositol-4,5-bisphosphate 3-kinase catalytic subunit beta; catalytic subunit of phosphoinositide-3-kinase (PI3K)

Target	RNE/ Fold Change	P	Gene Name and Description of Activity
	2.89/2.89	0.21	
	3.60/3.60	0.19	
Prkaa1	0.50/−2.01	0.01	Protein kinase AMP-activated, alpha 1 catalytic subunit catalytic subunit of AMPK
	0.77/−1.30	0.04	
	0.75/−1.33	0.04	
Prkab1	1.60/1.60	0.0001	Non-catalytic subunit of AMPK; beta-1 non-catalytic subunit
	0.85/−1.18	0.02	
	1.58/1.58	0.0001	
Prkag2	0.49/−2.03	0.01	Gamma-2 non-catalytic subunit of AMPK
	0.79/−1.27	0.05	
	1.16/1.16	0.11	
Pten	0.62/−1.61	0.01	Phosphate and tensin homolog, a phosphatidylinositol-3,4,5-triphosphate phosphatase. Dephosphorylates phosphoinositide substrates
	0.45/−2.21	0.01	
	0.98/−1.02	0.78	
Rheb	0.59/−1.68	0.0001	Ras homolog enriched in brain, a member of the GTPase superfamily.
	0.73/−1.38	0.01	Involved in regulation of growth and the cell cycle in the insulin/TOR/S6K pathway.
	0.74/−1.34	0.0001	
Rhoa	0.96/−1.04	0.01	Ras homolog family member a; component of the Rho family of GTPases
	0.72/−1.40	0.02	
	0.87/−1.15	0.08	
Rps6ka1	2.55/2.55	0.03	Ribosomal protein S6 kinase polypeptide 1; phosphorylates members of the MAPK pathway (mitogen activated protein kinase)

Biochim Biophys Acta. Author manuscript; available in PMC 2018 January 01.

Target	RNE/ Fold Change	P	Gene Name and Description of Activity
	1.12/1.12	0.40	
	1.40/1.40	0.06	
Rraga	0.81/−1.23	0.01	Ras-related GTP binding protein A; active in mTOR signaling
	0.42/−2.36	0.0001	
	0.97/−1.04	0.63	
Rragd	4.04/4.04	0.07	Ras-related GTP binding protein D; a G-protein (guanine nucleotide-binding protein) engaged in mTOR signaling
	23.10/23.10	0.06	
	1.32/1.32	0.60	
Sgk1	5.04/5.04	0.0001	Serum/glucocorticoid-regulated kinase 1; a ser/thr kinase involved in the cellular stress response
	3.78/3.78	0.0001	
	1.13/1.13	0.20	
Tsc1	0.75/−1.34	0.04	Tuberous sclerosis 1 gene; a growth inhibitory protein that stabilizes tuberin
	0.45/−2.21	0.0001	
	0.84/−1.19	0.22	
Ulk2	0.29/−3.50	0.01	Unc-51 like autophagy activating kinase 2; a ser/thr kinase active in axonal elongation
	0.39/−2.59	0.03	
	0.56/−1.80	0.04	

RNE, relative normalized expression; for each gene, the first row represents untreated *aldh5a1*$^{-/-}$ mice, the middle row *aldh5a1*$^{-/-}$ mice who had received Torin 1, and the final row *aldh5a1*$^{-/-}$ mice treated with Torin 2

Table 2

Liver expression of oxidative damage and antioxidant-activity related genes

Target	RNE/ Fold Change	P	Gene Name and Description of Activity
Akr1c18	0.04/−26.87	0.01	Aldo-keto reductase family 1, member c18; member of the aldo-keto reductase superfamily; metabolizes prostaglandin D2, a marker of oxidative stress.
	0.00/594.8	0.01	
	0.00/−371.1	0.01	
Aldh1a1	0.13/−7.50	0.01	Aldehyde dehydrogenase 1, member A1; active in ethanol and retinol (vitamin A) metabolism
	0.62/−1.62	0.03	
	1.19/1.19	0.11	
Casp3	0.42/−2.40	0.01	Member of the cysteine-aspartic acid protease family; central role in cellular apoptosis
	0.14/−7.30	0.0001	
	0.77/−1.30	0.08	
Ddit3	5.91/5.91	0.0001	Member CCAAT/enhancer binding protein (C/EBP) family of transcription factors; activated by endoplasmic reticulum stress, promoting apoptosis
	0.61/−1.64	0.01	
	1.43/1.43	0.11	
Dusp1	3.69/3.69	0.01	Dual specificity phosphatase 1; induced by oxidative and heat stress
	1.15/1.15	0.63	
	2.60/2.60	0.04	
Snca	0.29/−3.42	0.01	Synuclein, alpha; inhibitorof phospholipase D2; active in the pathogenesis of Parkinson disease
	0.41/−2.45	0.0001	
	0.09/−11.63	0.0001	
Cat	0.48/−2.08	0.01	Catalase; localized in the peroxisome; metabolizes hydrogen peroxide to water and molecular oxygen

Target	RNE/ Fold Change	P	Gene Name and Description of Activity
	0.49/−2.03	0.01	
	1.30/1.30	0.14	
Gpx1	0.59/−1.69	0.02	Glutathione peroxidase 1; involved in detoxification of hydrogen peroxide
	0.61/−1.63	0.02	
	1.33/1.33	0.01	
Gpx3	2.18/2.18	0.01	Glutathione peroxidase 3
	7.32/7.32	0.0001	
	1.13/1.13	0.36	
Gpx6	0.24/−4.24	0.10	Glutathione peroxidase 6
	0.62/−1.60	0.34	
	1.56/1.56	0.22	
Gpx7	0.19/−5.24	0.02	Glutathione peroxidase 7
	0.33/−3.02	0.04	
	0.31/−3.24	0.03	
Gstm	0.32/−3.11	0.0001	Glutathione-*S*-transferase mu 2 (muscle); detoxifies electrophilic compounds via conjugation with glutathione
	0.24/−4.21	0.0001	
	0.43/−2.35	0.02	
Gstt1	0.33/−3.02	0.0001	Glutathione-S-transferase theta
	0.46/−2.19	0.01	
	0.78/−1.28	0.04	
Prdx1	0.40/−2.51	0.01	Peroxiredoxin 1; antioxidant enzyme metabolizing hydrogen peroxide and other alkylhydroperoxides

Biochim Biophys Acta. Author manuscript; available in PMC 2018 January 01.

Target	RNE/ Fold Change	P	Gene Name and Description of Activity
	0.52/−1.92	0.0001	
	0.55/−1.81	0.01	
Prdx2	0.58/−1.73	0.01	Peroxiredoxin 2
	0.96/−1.04	0.54	
	0.99/−1.01	0.90	
Prdx4	0.35/−2.88	0.0001	Peroxiredoxin 4
	0.27/−3.77	0.0001	
	0.49/−2.05	0.01	
Prdx5	0.63/−1.58	0.01	Peroxiredoxin 5; interacts with peroxisome receptor 1
	0.75/−1.34	0.01	
	0.81/−1.23	0.02	
Prdx6	0.63/−1.59	0.02	Peroxiredoxin 6
	0.81/−1.23	0.02	
	1.29/1.29	0.08	
Sod1	0.61/−1.65	0.03	Superoxide dismutase 1, soluble; involved in clearing superoxide radicals
	0.87/−1.15	0.10	
	0.91/−1.10	0.42	
Sod2	0.61/−1.65	0.05	Superoxide dismutase 2, mitochondrial; metabolizes superoxide radicals radicals to hydrogen peroxide and molecular oxygen
	0.89/−1.12	0.51	
	0.93/−1.07	0.67	
Sod3	0.67/−1.50	0.03	Superoxide dismutase 3, extracellular

Target	RNE/ Fold Change	P	Gene Name and Description of Activity
	0.43/−2.34	0.0001	
	1.19/1.19	0.12	

RNE, relative normalized expression; for each gene, the first row represents untreated *aldh5a1*$^{-/-}$ mice, the middle row *aldh5a1*$^{-/-}$ mice treated with Torin 1, and the final row *aldh5a1*$^{-/-}$ mice treated with Torin 2